MYU Tokyo

S & M 4047

# Lifetime Prediction and Preventive Maintenance Strategy for an Automotive Belt Applied to Internet of Things

Shang-Kuo Yang, Yi-Ting Tsai, and Kai-Jung Chen*

Department of Mechanical Engineering, National Chin Yi University of Technology, Taichung 41170, Taiwan, R.O.C.

(Received February 6, 2025; accepted May 12, 2025)

***Keywords:*** automotive belt, predictive maintenance, curve fitting, failure prediction, Internet of Things

The failure of automotive belts in vehicle transmission systems can result in severe mechanical disruptions. However, conventional time-based maintenance strategies lack precision, often leading to either premature replacements or unexpected failures. We propose a condition-based predictive maintenance strategy that utilizes the real-time monitoring of belt wear to enhance the accuracy of lifespan estimation. The primary objective of this study is to overcome the limitations of time-based maintenance by developing a data-driven predictive model that accurately estimates the remaining lifespan of automotive belts on the basis of thickness-wear progression. A nine-month experimental study was conducted, during which an automotive belt's thickness wear was continuously monitored using a high-precision displacement sensor. The collected data was processed using MATLAB, where curve fitting was performed, leading to the derivation of an eighth-order polynomial equation by the least squares method. This mathematical model serves as the foundation for predictive analysis, enabling accurate estimations of belt-wear progression and failure timelines. By leveraging this predictive model, maintenance planning can be significantly improved, reducing the risk of unexpected failures while optimizing replacement schedules and lowering operational costs. Furthermore, in this study, we present a novel condition-based maintenance framework that is compatible with Internet of Things (IoT) applications, facilitating real-time diagnostics and smart predictive maintenance in automotive engineering.

## 1. Introduction

Automotive belts are critical components in vehicle transmission systems, responsible for efficiently transferring power from the transmission shaft to various driving elements via friction-based mechanisms. These belts engage with gears of various sizes, enabling essential energy conversion between torque and rotational speed, which is necessary for the proper functioning of mechanical devices. For instance, reducing the high rotational speed of a motor to a lower speed suitable for driving devices often requires this energy conversion. A failure in the

*Corresponding author: e-mail: hskchen5@ncut.edu.tw
https://doi.org/10.18494/SAM5595

ISSN 0914-4935 © MYU K.K.
https://myukk.org/

automotive belt can lead to significant disruptions in the transmission system, underscoring the importance of accurate belt failure prediction.

Traditionally, the maintenance of automotive belts has relied on time-based strategies, where the average lifespan of a belt is used as a reference for replacement. However, this method has inherent limitations: belts may be replaced prematurely, leading to unnecessary costs, or, conversely, may fail unexpectedly if their lifespan is shorter than the estimated average. To address these limitations, condition-based maintenance (CBM) strategies have been proposed as a more effective approach. CBM involves real-time monitoring of the belt's operational condition using sensors to track wear and degradation; this enables predictive maintenance instead of arbitrary scheduled replacements.

In this study, we utilize a CD3-80N displacement sensor to measure the thickness variation of automotive belts, aiming to identify key indicators of belt failure. The collected sensor data is processed using MATLAB-based curve-fitting algorithms, where an eighth-order polynomial equation is derived by the least squares method. This predictive model provides a data-driven approach to estimate the remaining lifespan of automotive belts with high accuracy. By integrating this method with Internet of Things (IoT) technology, real-time monitoring and remote predictive maintenance become feasible, reducing unexpected failures and improving the reliability of vehicle transmission systems.

As automotive belts are consumable components, regular maintenance or replacement is essential to ensure the continued functionality of vehicle systems. Various methodologies for predicting belt lifespan have been explored in numerous studies. For example, Kirjanów-Błażej *et al.* used ultrasonic sensors to assess wear on drive belts, mapping changes in belt areas corresponding to different wear stages through software analysis.(1) Jayatilleka and Okogbaa conducted accelerated life testing under multiple stress levels on transmission belts, utilizing Weibull distribution models to estimate reliability over time.(2) Research by Fritzson(3) and Li and Xin(4) further advanced the field by developing tension-speed charts based on the experimental analysis of V-belt fatigue, in which finite element analysis (FEA) was integrated to predict belt failure by correlating stress distribution with operational parameters.

Despite these advancements, most current methods rely on time-based maintenance or offline analysis and hence lack real-time predictive capabilities. We propose a sensor-integrated, IoT-enabled, CBM strategy, focusing on the real-time assessment of belt thickness wear in the driving system. The developed predictive failure model enables proactive maintenance, which will minimize downtime and reduce overall maintenance costs. By integrating sensor data with MATLAB-driven machine learning models, this approach enhances the accuracy and practicality of belt failure prediction, offering a more efficient, data-driven maintenance solution for automotive applications.

## 2. Automotive Belt and Its Fatigue

### 2.1 Structure and materials

Timing belts are essential components in automotive transmission systems. They are composed primarily of two key elements: tensile cords, which bear the torque load, and a polymer matrix, which forms the belt's teeth and encapsulates the cords.(5) The tensile cords, typically made from glass fiber or polyester, provide high tensile strength to withstand the significant loads encountered during operation. The polymer matrix, usually composed of rubber or polyurethane (PU), offers the flexibility and durability required for the belt's continuous operation.

The integration of sensor-based monitoring systems into automotive belts has enabled the real-time tracking of belt wear and material degradation, contributing to enhanced predictive maintenance. For instance, displacement sensors can monitor belt elongation and wear patterns, while infrared thermography sensors can detect temperature variations associated with material fatigue. Such sensor-based assessments are crucial in identifying early-stage failures before catastrophic damage occurs.

Figure 1 illustrates the structure of a timing belt, showcasing its multilayered composition, where each layer plays a critical role in ensuring durability and functionality. The outer cover layer, made from wear-resistant materials such as nylon or rubber, acts as a protective shield against external damage, including abrasion and environmental factors. Beneath this, the base layer, typically rubber or PU, provides the flexibility and resilience that allows the belt to sustain prolonged mechanical stress. The tooth profile layer ensures efficient power transmission by engaging with gears, while the innermost reinforcement layer, composed of fiberglass or polyester tensile cords, maintains the belt's structural integrity under high torque conditions. This multilayer composite design optimizes strength, flexibility, and durability, ensuring reliable performance in demanding automotive applications.

The composite nature of timing belts is engineered to leverage the combined properties of their constituent materials, resulting in a final product with high strength, light weight, and enhanced wear resistance.(6) However, during extended operation, internal stresses can induce delamination at the interfaces of different layers owing to variations in Poisson's ratio, which arise from differing fiber orientations within the material layers.

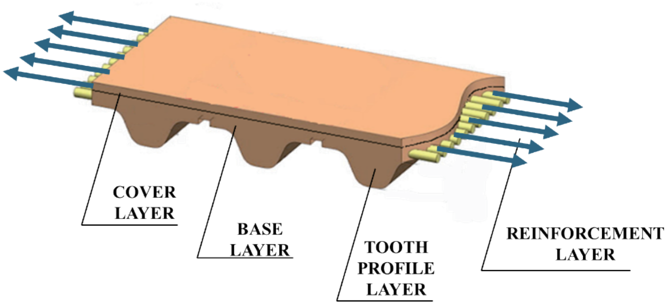


Fig. 1. (Color online) Structure of a timing belt.

Delamination, particularly pronounced at the edges of the belt, is critical because it reduces the belt's mechanical strength and structural stability. Figure 2 illustrates this phenomenon, where the disparity in Poisson's ratio between the layers causes them to separate under stress. This delamination often initiates at the interface between two different materials or within a single material layer that experiences differential deformation.

In addition to delamination, the edge effect is another significant concern in composite materials. Figure 3 depicts the force distribution at the edge of a composite material, which can lead to stress concentration and potential failure. The edge effect arises because the material at the edge undergoes different stress distributions compared with the core regions of the belt. This discrepancy can result in localized stress concentrations, causing the edges to either bulge outward or contract inward, which may ultimately precipitate cracks and other forms of material degradation.

The effective management of these structural weaknesses is crucial in the design and manufacturing of composite materials, especially for high-stress applications such as automotive belts. Advanced manufacturing techniques, such as fiber alignment optimization and reinforced bonding treatments, can help mitigate these failure mechanisms, thereby improving the belt's operational longevity and reliability.

Fig. 2. (Color online) Delamination in composite materials owing to variations in Poisson's ratio.

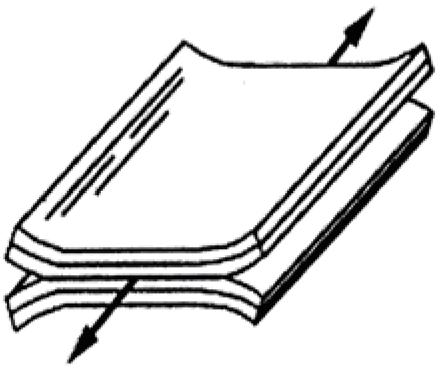

Fig. 3. Force distribution at the edge of a composite material.

### 2.2 Creep

Creep refers to the gradual deformation or deterioration of materials over extended periods under constant mechanical stress.[7] This phenomenon is particularly critical in high-stress applications, such as automotive belts, where materials are continuously subjected to tensile and compressive forces. Over time, creep can significantly degrade the performance of mechanical components, reducing efficiency, accelerating wear, and potentially leading to catastrophic failure.

To mitigate the risks associated with creep, modern sensor technologies have been integrated into automotive belts to provide real-time monitoring of material deformation. For instance, strain gauges and fiber optic sensors are employed to detect microlevel elongation, while infrared thermal sensors can track temperature variations that accelerate creep degradation. These sensor-based monitoring techniques allow for the early detection of abnormal creep behavior, enabling predictive maintenance strategies that extend the lifespan of automotive belts and prevent unexpected failures.

The creep phenomenon is generally categorized into three distinct stages, each characterized by different deformation rates, as illustrated in Fig. 4. In the primary creep phase (segment AB), the material undergoes an initial rapid deformation immediately after the application of stress. This initial deformation occurs as the material's internal structure realigns in response to the applied load. As time progresses, the deformation rate decreases, indicating that the material is adapting to stress and developing resistance to further deformation. This transition leads to the secondary creep phase. The secondary creep phase (segment BC) is characterized by a relatively steady deformation rate and is also known as the steady-state creep phase. This stage typically lasts the longest, during which the material deforms at a constant rate as it reaches a dynamic equilibrium between applied stress and material resistance. Intrinsic material properties and

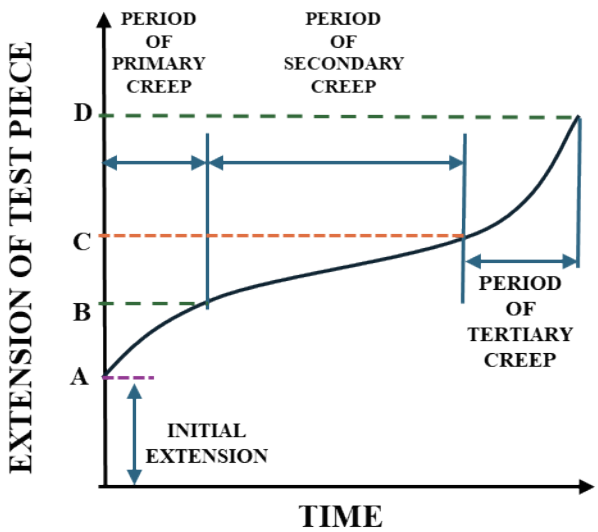


Fig. 4. (Color online) Three stages of creep.

external environmental conditions, including temperature, humidity, and exposure to oxidative elements, strongly affect the duration of secondary creep. The final phase, tertiary creep (segment CD), occurs when the deformation rate accelerates rapidly, ultimately leading to structural failure. This phase is characterized by the progressive accumulation of microscopic damage, including the formation and propagation of microcracks, voids, and grain boundary sliding. As these defects grow, the material loses its structural integrity, culminating in rupture or fracture, marking the end of its functional service life under the given stress conditions.

The duration and characteristics of these creep stages depend on multiple factors, including the material's composition, applied stress level, and operating environment. Studies have shown that materials exposed to high-temperature conditions are particularly susceptible to creep.[8–10] In such scenarios, even materials with lower elastic limits may experience gradual plastic deformation when subjected to continuous stress.

Prolonged exposure to elevated temperatures exacerbates creep-induced material degradation, making thermal management a critical factor in the design and operation of automotive belts. Advanced cooling systems, heat-resistant coatings, and optimized material selection play a crucial role in reducing the impact of creep and extending belt longevity. Additionally, real-time creep monitoring using embedded sensors provides valuable data for predictive analytics, helping engineers refine maintenance schedules and improve the reliability of automotive systems.

Overall, Fig. 4 provides a comprehensive overview of creep behavior, demonstrating how different creep phases affect material durability over time. Understanding these stages is critical for designing materials and components that can withstand prolonged stress, particularly in high-performance applications such as automotive belts, where creep-induced elongation and mechanical fatigue can lead to severe performance degradation or failure.

### 2.3 Fatigue damage

Fatigue damage refers to the progressive and localized structural deterioration that occurs when a material is subjected to cyclic loading. Over time, the repeated application of loads leads to the initiation and propagation of cracks, ultimately resulting in material failure. Studies have revealed that fatigue damage is exacerbated by the combined effects of mechanical loading and environmental factors, such as corrosion, thermal fluctuations, and humidity exposure.[11,12] These factors accelerate crack initiation and propagation, significantly reducing the lifespan of automotive components.

Recent advancements in sensor technology have enabled the real-time monitoring of fatigue damage in automotive belts. For instance, acoustic emission sensors detect microcrack formation, while strain gauges and fiber optic sensors measure stress variations during cyclic loading. Additionally, infrared thermography sensors can track localized heat generation due to internal friction, providing valuable insights into fatigue-induced material degradation. These sensor-based approaches allow for early fault detection, facilitating predictive maintenance strategies that help prevent unexpected failures in critical automotive applications.

The fatigue damage process is generally divided into three distinct stages: crack initiation, propagation, and failure.

- Crack Initiation: Small cracks begin to form at high-stress concentration points, such as material defects, surface roughness, or areas subjected to repeated stress cycles. This stage is critical because the initial formation of a crack lays the foundation for further damage
- Crack Propagation: As cyclic loading continues, existing cracks extend, marking the transition to the propagation stage. Several factors affect the crack growth rate, including the magnitude of applied stress, loading frequency, and environmental conditions. Stress concentration at the crack tip intensifies as the crack elongates, accelerating its propagation rate. This phase is crucial in determining the remaining service life of the material
- Catastrophic Failure: When a crack reaches a critical size, the material can no longer sustain the applied stress, leading to sudden and often unpredictable fracture. In critical automotive components such as timing belts, catastrophic failure can result in severe mechanical damage or even hazardous operational failures.

Figure 5 illustrates the crack growth curve, depicting the relationship between crack size and the number of stress cycles (or time) in a material subjected to cyclic loading. Initially, during the crack initiation phase, the increase in crack size is minimal as microcracks form at high-stress points. These microcracks, often imperceptible at first, gradually accumulate as the material undergoes cyclic loading. During the crack propagation phase, the crack growth rate increases steadily, as shown by the upward trend in Fig. 5. The stress concentration at the crack tip increases as the crack extends, resulting in a positive feedback loop where the crack expands at an accelerated rate over time. In the final failure phase, the crack reaches a critical threshold, leading to rapid propagation and catastrophic failure. The steep rise of the curve towards the end of the graph highlights the exponential nature of crack growth before failure. Thus, Fig. 5 serves as a crucial reference for understanding how fatigue damage progresses under cyclic stress conditions. By utilizing sensor-based real-time monitoring, engineers can predict the lifespan of materials and components, allowing for timely maintenance or replacement before catastrophic failure occurs. This predictive approach is particularly valuable in high-performance automotive applications, where fatigue-induced failures can lead to significant operational risks.

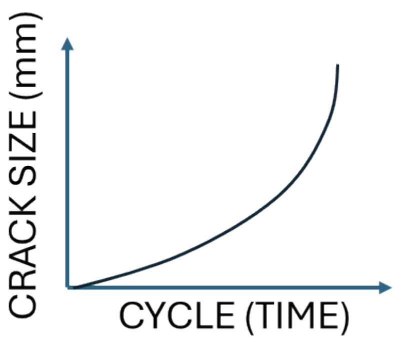


Fig. 5. Crack growth curve.

### 2.4 Possible causes of timing belt breakage

Timing belt breakage is primarily caused by two main factors: fatigue damage from cyclical loading and surface damage that leads to failure. Fatigue damage occurs as a result of the repeated application of loads below the material's yield point. Over time, this repeated loading generates small cracks that propagate through the material, eventually leading to catastrophic failure. These fatigue cracks often originate from surface imperfections, such as scratches, inspection marks, or other minor defects, which act as stress concentrators. These imperfections increase the local stress levels and serve as initiation points for fatigue cracks. Additionally, residual stresses on the belt surface, which may result from manufacturing processes or operational conditions, can further contribute to the risk of fatigue damage.

Timing belts can fail under various loading conditions, including high-frequency, low-energy loading or low-frequency, high-energy loading. High-frequency, low-energy loading involves frequent but relatively low-intensity stress cycles that can gradually weaken the material over time. In contrast, low-frequency, high-energy loading subjects the belt to fewer but more intense stress cycles, which can lead to more immediate damage. The sequence of belt failure typically involves several stages: lattice dislocation, creep, belt hardening, fatigue crack formation, stress concentration at the crack, and ultimately, catastrophic failure. Lattice dislocation refers to the movement of atoms within the material's crystal structure, which can weaken the material over time. Creep involves the slow, time-dependent deformation of the belt material under constant stress, which can lead to belt hardening—a process where the material becomes more brittle and less ductile. As the material hardens, it becomes more susceptible to fatigue crack formation. These cracks create stress concentrations, accelerating the crack propagation and eventually leading to sudden, catastrophic failure. Thus, to prevent timing belt breakage and ensure operational reliability, it is essential to address both fatigue damage and surface damage. This involves careful monitoring of the belt's condition, identifying and mitigating potential sources of surface imperfections, and managing the operational stresses to which the belt is subjected. By understanding the causes and mechanisms of belt failure, engineers can design more robust timing belts and develop maintenance strategies that reduce the likelihood of unexpected failures.

## 3. Experimental Setup

The primary aim of this experiment is to investigate the fatigue wear and breakage behavior of automotive belts under cyclic loading while exposed to elevated temperatures. During prolonged operation, automotive belts are subjected to various stresses, particularly in high-temperature environments, which significantly affect their reliability and durability. Therefore, understanding their failure mechanisms is crucial for enhancing belt performance and lifespan. This experiment was designed to simulate real-world conditions by continuously applying loads, heating, and monitoring the wear on the belt's surface and structure over time. The results of this study will provide valuable insights into the factors contributing to belt failure and help develop preventive maintenance strategies to ensure longer service life.

The experimental setup was specifically built to enable long-term, nonstop testing of automotive belts. The setup replicates real-life vehicle conditions to which automotive belts are subjected by simulating working environment temperatures and cyclic loading conditions. The entire experimental process is carefully monitored and controlled, with data collected at regular intervals to assess both belt wear and the formation of cracks. This continuous data collection allows an in-depth analysis of how automotive belts degrade under stress.

### 3.1 Experimental equipment

The hardware setup used in this experiment is designed to replicate real-world conditions, focusing on environments where automotive belts endure continuous cyclic loading and high temperatures. The experimental station operates continuously for 24 h, allowing for long-term testing and observation of the automotive belt performance under stress. The central aspect of the experiment involves prolonged exposure to elevated temperatures, a key factor contributing to belt thickness wear and eventual failure. Heating elements exposed the belts and passive components within the transmission system to sustained high temperatures, ensuring the experiment simulated actual vehicle operation conditions.

As shown in Fig. 6, the experimental station integrates heating and mechanical drive systems. The automotive belt used in the experiment is BANDO model 3410 with a rectangular profile fitting (RPF) tooth profile, and dimensions of 1015 mm in length, 13 mm in width, and 8.8 mm in thickness. These specifications represent a typical automotive belt commonly used in vehicle transmission systems, providing a representative model for studying thickness wear and failure under high-temperature conditions. During the experiment, the belt is subjected to cyclic loads and heat to observe its wear progression and failure behavior over time.

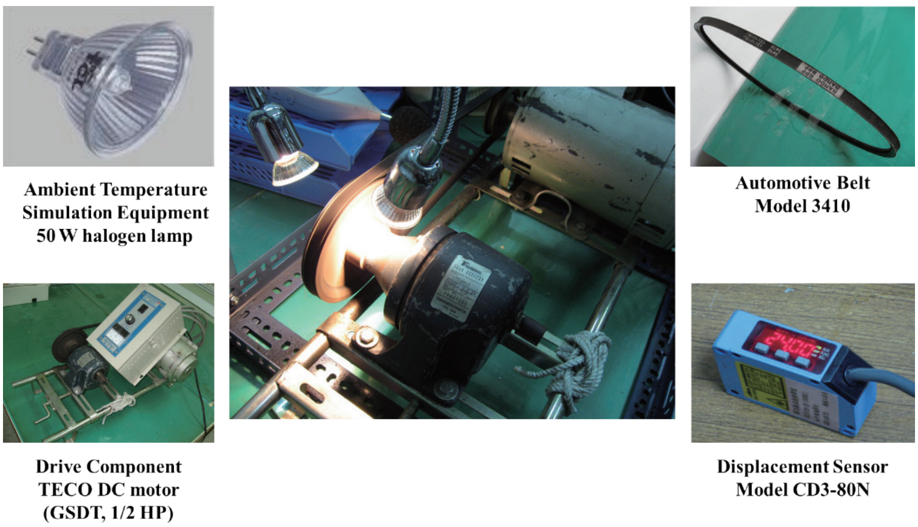


Fig. 6. (Color online) Heated experimental station.

The heat necessary for the simulation is provided by a 110 V, 50 W halogen lamp, which maintains a high-temperature environment for both the belt and the passive components of the transmission system. This continuous heating process mirrors the intense conditions in real-world automotive applications. As the belt operates in this high-temperature environment, the TECO DC motor (GSDT, 1/2 HP) runs the belt at a constant speed of 1400 rpm, generating the cyclic stress needed to simulate typical vehicle operation.

To monitor the belt's condition throughout the experiment, a displacement sensor (model CD3-80N) is used to measure the belt's deformation and thickness changes. This sensor, equipped with a red laser diode (wavelength 650 nm), provides precise measurements within a range of 80±15 mm, capturing even minute changes in the belt's thickness. The sensor's 10 μm resolution ensures high accuracy, allowing researchers to monitor the belt's thickness-wear progression and detect early signs of potential failure.

By combining heating, cyclic loading, and precise monitoring, this experimental setup effectively replicates the harsh conditions that automotive belts face in real-world applications. The continuous 24-h operation of the experiment ensures sufficient data collection over time, offering valuable insights into the belt's behavior under stress. These insights contribute to developing more durable automotive belts capable of withstanding high-temperature and high-stress environments.

Overall, all devices of the setup are described as follows.

(1) Ambient Temperature Simulation Equipment: A 110 V, 50 W halogen lamp heats the automotive belt and passive components in the transmission system, allowing the belt to operate for extended periods in harsh, high-temperature environments simulating real-life vehicle operating conditions.
(2) Automotive Belt: The BANDO model 3410 belt has a RPF tooth profile, length of 1015 mm, width of 13 mm, and thickness of 8.8 mm.
(3) Drive Component: A TECO DC motor (GSDT, 1/2 HP) is the driving motor for the belt and is run at 1400 rpm to simulate real-life cyclic stress conditions.
(4) Displacement Sensor: The displacement sensor (model CD3-80N) features a red laser diode with 650 nm wavelength, a measurement range of 80±15 mm, and a maximum output power of 1 mW. The sensor has a resolution of 10 μm and converts thickness changes into current signals for real-time analysis.

### 3.2 Data collection and analysis

In this experiment, data collection focuses on continuously monitoring the deformation and thickness wear of the automotive belt over an extended period. The displacement sensor is used to convert the belt's displacement into electrical current signals that reflect the belt's thickness variations. These signals are critical for tracking the progressive thickness wear of the belt and identifying potential points of failure, especially under high-temperature and cyclic loading conditions.

The displacement sensor is programmed to take measurements every five minutes, ensuring that detailed and continuous data is gathered. Each five-minute interval produces one current signal, which represents the belt's thickness at that point in time. Over the course of a single day, 288 signals are recorded, and with the experiment running continuously for 273 days, a total of 78624 data points are accumulated.

The data collected from the displacement sensor provides a comprehensive view of the belt's thickness-wear progression over time. This data is analyzed to identify patterns and changes in the belt's thickness, allowing researchers to detect early signs of damage, such as small decreases in thickness that could indicate the onset of fatigue or crack formation. As the belt is subjected to cyclic loading and heating, gradual wear is expected to occur, and the data analysis reveals how quickly or slowly this wear progresses.

In addition to monitoring general thickness wear, the data is used to observe specific failure characteristics of the belt. For instance, sudden changes in thickness measurements may signal the development of cracks or significant surface damage. By examining these anomalies in the data, researchers can determine when and how the belt begins to fail. This real-time monitoring and analysis provide crucial insights into the durability of the belt and the factors that lead to its eventual breakdown.

To ensure the accuracy of the collected data, a zero-point correction is applied at the start of the experiment. This correction accounts for any initial calibration errors in the sensor and ensures that the thickness measurements accurately reflect the belt's wear over time. The corrected data is then used to calculate both cumulative and monthly thickness wear, providing essential metrics for assessing the belt's performance and predicting when it will fail.

The data collected from the 273-day experiment helps in the evaluation of the overall performance of the belt and provides information for future improvements in belt design. By understanding the progression of thickness wear and identifying the key factors leading to failure, the findings from this analysis can contribute to the development of more durable and reliable automotive belts that can withstand prolonged operation in high-temperature, high-stress environments.

### 3.3 Zero-point correction of thickness wear

The surface of the testing belt is not entirely smooth but contains small protrusions, as shown in Fig. 7. These surface irregularities create challenges in accurately measuring the belt's thickness. To address this issue, the following assumptions are made to ensure consistency in the thickness measurement of the belt:

(1) Uniform Distribution of Protrusions: The protrusions on the belt's surface are assumed to be uniformly distributed across the entire surface.

(2) Equal Area of Plane and Protrusions: The total area of the belt's flat plane is considered equal to the total area of the protrusions, ensuring a balanced measurement.

(3) Equal Probability of Light Signal Emission: The probability of the light measurement signal being emitted from either the plane of the belt or the protrusions is assumed to be equal. This ensures that no part of the belt's surface is favored over another in the measurement process.

(4) Midpoint as Zero-Point: The midpoint between the belt's plane and the protrusions' highest point is designated as the absolute zero point for the measurement.

Fig. 7. (Color online) Close-up of plane and protrusions on the belt surface.

(5) Minimal Impact of Light Scattering: Light scattering phenomena are assumed to have a minimal impact on the accuracy of the measurement values, ensuring that the results are not significantly affected by surface reflection.

As illustrated in Fig. 7, these assumptions allow for a standardized approach to measuring the belt's thickness, despite the presence of surface irregularities.

All data collected during the experiment undergo zero-point correction at the start to avoid errors and ensure accurate results. This correction process adjusts the initial measurements to account for any discrepancies caused by the belt's surface texture, ensuring that the subsequent measurements reflect the actual wear progression of the belt over time. The monthly thickness wear of the belt before and after the zero-point correction is presented in Tables 1 and 2, respectively. Additionally, the thickness-wear data is visualized in Figs. 8 and 9, which show the monthly and cumulative thickness wear before and after calibration. These corrections provide a more accurate depiction of the belt's thickness-wear progression throughout the experiment.

Through the course of the experiment, it was observed that the cumulative thickness wear of the belt increased proportionally with driving time. When the belt's thickness wear reached approximately 1.25 mm, the first complete crack and several incomplete cracks began to appear, as shown in Fig. 10. Upon reaching a cumulative thickness wear of 2.828 mm, the belt failed by rupturing. These findings indicate a clear correlation between cumulative thickness wear and the occurrence of belt failure, providing more informative insights for understanding the wear threshold that leads to automotive belt failure.

## 4. Methods for Predicting Belt Breakage

The ability to predict the point at which an automotive belt will fail is crucial for developing preventive maintenance strategies that can extend the service life of the belt and prevent unexpected breakdowns. By understanding the relationship between thickness wear, operating conditions, and failure points, it is possible to predict when a belt is approaching a critical thickness-wear threshold and the schedule maintenance accordingly. In this study, various methods are employed to analyze the wear progression of automotive belts and predict their

Table 1
Belt thickness and wear before calibration.

| Date | Cumulative thickness wear (mm) | Monthly thickness wear (mm) |
|---|---|---|
| September 2022 | −0.056 | 0 |
| October 2022 | 0.332 | 0.388 |
| November 2022 | 0.914 | 0.582 |
| December 2022 | 1.026 | 0.112 |
| January 2023 | 1.114 | 0.088 |
| February 2023 | 1.202 | 0.088 |
| March 2023 | 1.420 | 0.218 |
| April 2023 | 2.107 | 0.687 |
| May 2023 | 2.716 | 0.608 |

Table 2
Belt thickness and wear after calibration.

| Date | Cumulative thickness wear (mm) | Monthly thickness wear (mm) |
|---|---|---|
| September 2022 | 0 | 0 |
| October 2022 | 0.388 | 0.388 |
| November 2022 | 0.97 | 0.582 |
| December 2022 | 1.082 | 0.112 |
| January 2023 | 1.17 | 0.088 |
| February 2023 | 1.258 | 0.088 |
| March 2023 | 1.533 | 0.274 |
| April 2023 | 2.163 | 0.687 |
| May 2023 | 2.828 | 0.608 |

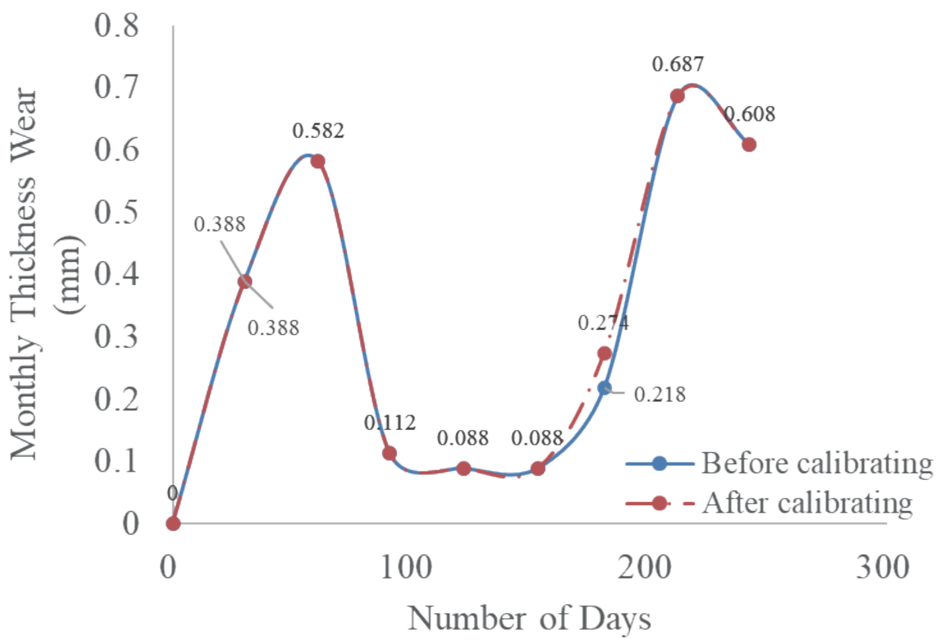


Fig. 8. (Color online) Monthly thickness before and after correction.

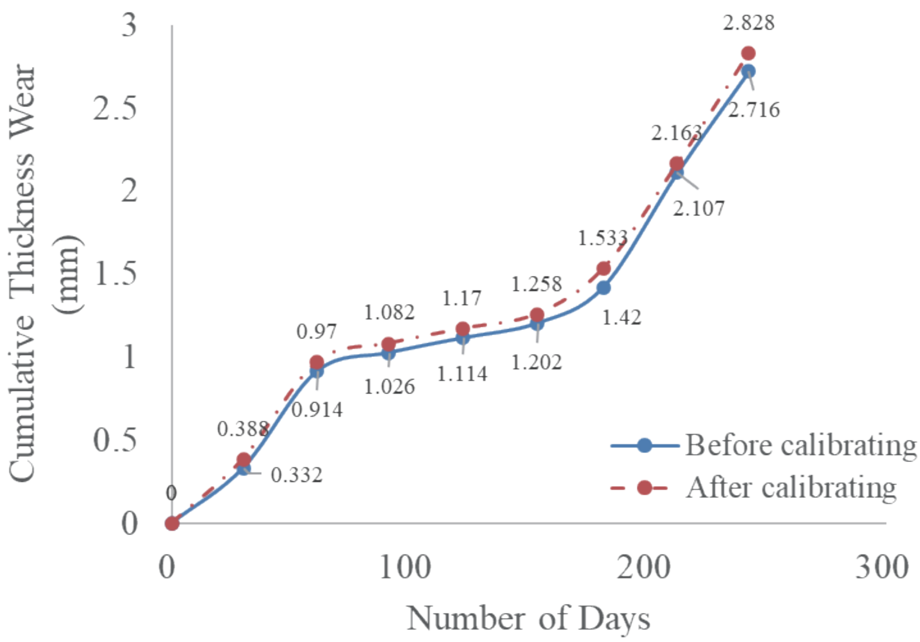


Fig. 9. (Color online) Cumulative thickness before and after correction.

Fig. 10. (Color online) First completed crack in testing belt.

breakage. These methods rely on real-time data collected during the experiment, including thickness measurements and crack formation. A predictive model can be constructed through statistical analysis and curve-fitting techniques to forecast the belt's remaining life before failure occurs.

Curve fitting is a statistical technique used to identify the best-fitting curve or line describing a data point set. It involves selecting a mathematical function or model and adjusting its parameters to minimize the differences between the predicted values and the actual observed values from the data. The curve fitting plays a crucial role in data analysis, as it allows for the establishment of a mathematical model based on a limited number of sample points, which can then be used for predictive analysis. In this study, curve fitting is employed to simulate the cumulative thickness wear of the automotive belt over time. By optimizing the equation using the least squares method, we develop a reliable model for predicting belt thickness wear and the eventual failure of the belt in dynamic vehicle systems.

To achieve this, MATLAB programming is used to simulate the experimental data and fit the curves using polynomial equations. The experimental data on cumulative thickness wear is substituted into the equation to compute the best-fitting curve, which is crucial for accurate predictions. The resulting equation, as shown in Eq. (1), is an eighth-order polynomial that accurately reflects the thickness-wear progression of the automotive belt,

$$Y = G_0 + G_1X^1 + G_2X^2 + G_3X^3 + G_4X^4 + G_5X^5 + G_6X^6 + G_7X^7 + G_8X^8, \tag{1}$$

where $Y$ represents the thickness wear, $X$ represents time, and $G_0$ to $G_8$ are the parameters of the equation listed in Table 3. These parameters are determined through the curve-fitting process and provide the basis for predicting the wear behavior of the belt over time. By inputting the measured cumulative thickness wear of the belt into this predictive equation, the remaining lifespan of the belt can be calculated, offering critical information for determining when maintenance should be performed. This predictive capability helps avoid unexpected failures by providing timely insights into the belt's condition.

With this equation, the monthly thickness wear and cumulative thickness wear can be calculated, as shown in Table 4, which also includes the corresponding reliability for each stage. As the belt wears over time, the reliability gradually decreases, eventually reaching 0% when the cumulative thickness wear approaches 2.828 mm, indicating belt failure.

A regression line represents the relationship between two variables in a scatterplot and summarizes how one variable predicts the other. The line is calculated using statistical methods such as least squares regression, which minimize the differences between the observed data points and the values predicted by the regression line. We apply the least squares method to fit the cumulative thickness-wear data, ensuring that the resulting curve minimizes the error between predicted and observed values. This technique provides a predictive model for the automotive belt's wear progression.

The least squares method calculates the best-fit curve by minimizing the sum of squared errors between the observed values and the values predicted using the equation.[13,14] Although the theoretical values derived from the curve-fitting process may not perfectly match the actual values, the method optimizes the total error across all data points. This error, computed for each moment, is squared and summed, and the process yields a total sum of least squares errors.

In this study, the eighth-order equation used for curve fitting produces a total sum of least squares errors of approximately 0.0033 mm, a minimal error within the acceptable range. This small error confirms the accuracy of the model and its reliability in predicting automotive belt thickness wear. The results show that the optimized equation can effectively forecast the remaining lifespan of the belt, allowing for better maintenance planning and prevention of unexpected belt failures.

Table 3
Parameter values used in the eighth-order equation simulation.

| Parameter | Value |
|---|---|
| $G_0$ | 10.88000000006060 |
| $G_1$ | −27.13375238108007 |
| $G_2$ | 25.69342718266406 |
| $G_3$ | −12.35379305562382 |
| $G_4$ | 3.43567743057783 |
| $G_5$ | −0.57583888889327 |
| $G_6$ | 0.05732430555606 |
| $G_7$ | −0.00311567460321 |
| $G_8$ | 0.00007108134921 |

Table 4
Calculated data and reliability.

| Month | Monthly thickness wear (mm) | Cumulative thickness wear (mm) | Reliability (%) |
|---|---|---|---|
| 1 | 0.0000 | 0.00 | 100.0 |
| 2 | 0.1372 | 0.3880 | 86.3 |
| 3 | 0.3430 | 0.9700 | 65.7 |
| 4 | 0.3830 | 1.0830 | 61.7 |
| 5 | 0.4141 | 1.1710 | 58.6 |
| 6 | 0.4452 | 1.2590 | 55.5 |
| 7 | 0.5421 | 1.5330 | 45.8 |
| 8 | 0.7850 | 2.2200 | 21.5 |
| 9 | 1.0000 | 2.8280 | 0.0 |

## 5. Discussion

In this study, we integrated a key parameter—automotive belt thickness variation—with life analysis to conduct a comprehensive failure analysis of automotive belts. The V-belt was selected as the primary subject for investigating the prediction of dynamic vehicle transmission belt breakage. Through experimentation, it was discovered that when the thickness wear of the automotive belt reaches approximately 1.25 mm, the first complete crack and several incomplete cracks begin to appear. The collected data were systematically processed and summarized, and utilizing the curve-fitting function in MATLAB, we derived an eighth-order equation. The actual wear data were compared with the theoretical values, and the least squares method was applied to optimize the predictive model.

It is important to note that there is a time interval between the initial occurrence of belt failure and the point where the belt becomes completely unusable. During this period, the driver has the opportunity to take the vehicle to a service center for maintenance. This concept is similar to how a motorcycle's engine oil warning light signals low oil levels without necessarily indicating that the engine is critically low on oil or at risk of damage. Instead, it serves as a timely reminder to replace the oil.

To provide vehicle owners with a clear understanding of the remaining lifespan of their automotive belts, the data collected from thickness measurements can be input into the predictive equation. The vehicle's onboard computer system can then calculate the time remaining before the belt is expected to break and lose functionality. This predictive capability is instrumental in preventing unexpected belt failures, offering drivers the foresight needed to perform maintenance before critical damage occurs.

The results of this study provide valuable insights for implementing preventive maintenance strategies for automotive belts, allowing drivers to address potential issues before they escalate to critical failures that could render the vehicle inoperable.

While we focused on testing a single belt type in this study, the results apply to failure predictions for automotive belts with similar specifications. However, because of limitations in experimental facilities and equipment, we were unable to test other types of toothed belts. Therefore, future research is necessary to determine whether the failure characteristics observed in this study are universal across different belt models.

Moving forward, analysis can be expanded by incorporating tools such as the TES-1358 noise meter, which measures various frequencies and amplitudes generated by rotating belts. This can provide an additional parameter for enhancing the accuracy of automotive belt lifetime predictions.

Moreover, the results of this experiment can be integrated with satellite navigation systems. By using satellite navigation chips to monitor the operational status of the automotive belt and combining this information with GPS, drivers can be alerted to the nearest service center for maintenance before the belt fails. This will help achieve the goal of CBM, ensuring proactive vehicle care based on real-time belt conditions.

## 6. Conclusions

The results of the experiments revealed that when the thickness wear of the tested automotive belt reached approximately 1.25 mm, the first complete crack, along with several incomplete cracks, began to appear. As the wear progressed to 2.828 mm, the belt reached the end of its functional lifespan. The data collected during the experiments were systematically organized and analyzed, leading to the development of an eighth-order equation using the curve-fitting function in MATLAB. This predictive model allows drivers to input real-time thickness-wear data to assess the remaining lifespan of the belt accurately.

By utilizing this equation, drivers can proactively monitor the condition of their automotive belts, preventing sudden failures and unexpected ruptures. Moreover, this method enhances the efficiency of vehicle diagnostic systems, providing drivers with timely maintenance recommendations. With early identification of belt-wear issues, this approach helps resolve potential problems before they escalate into accidents or vehicle breakdowns, ultimately improving both safety and reliability in vehicle operation.

## References

1 A. Kirjanów-Błażej, L. Jurdziak, R. Błażej, and A. Rzeszowska: Measurement **214** (2023) 112744. https://doi.org/10.1016/j.measurement.2023.112744
2 S. Jayatilleka and G. Okogbaa: Annual Reliability and Maintainability Symp. **2003** (2003) 101.
3 D. Fritzson: ASME J. Mechanisms, Transmissions, and Automation in Design **111** (1989) 424. https://doi.org/10.1115/1.3259015
4 W. Li and Z. Xin: Int. J. Fatigue **111** (2018) 269. https://doi.org/10.1016/j.ijfatigue.2018.02.025
5 H. Zhu, W. D. Zhu, and W. Fan: J. Sound Vib. **491** (2021) 115759.
6 A. E. Krauklis, C. W. Karl, A. I. Gagani, and J. K. Jørgensen: J. Compos. Sci. **5** (2021) 28.

7 J. Betten: Creep Mechanics (Springer Science & Business Media, 2008).
8 G. W. Meetham: J. Materials Science **26** (1991) 853.
9 M. B. Ruggles-Wrenn, P. Koutsoukos, and S. S. Baek: J. Materials Science **43** (2008) 6734.
10 Y. Yamamoto, M. P. Brady, M. L. Santella, H. Bei, P. J. Maziasz, and B. A. Pint: Metall. Mater. Trans. A **42** (2011) 922.
11 P. Bortnowski, W. Kawalec, R. Król, and M. Ozdoba: Eng. Fail. Anal. **140** (2022) 106520.
12 Y. Huang, S. Li, G. Xiao, B. Chen, Y. He, and K. Song: Eng. Fail. Anal. **129** (2021) 105670.
13 M. Andrejiová and D. Marasová: Acta Montan. Slovaca **18** (2013) 77.
14 S. Karunendiran: Development of a New Model for the Prediction of Automotive Serpentine Belt Life (Ph. D. dissertation, University of Toronto, 2009).


## About the Authors


**Shang-Kuo Yang** received his B.S. (1982) and M.S. (1985) degrees in automatic control engineering from Feng Chia University, and his Ph.D. degree (1999) in mechanical engineering from National Chiao Tung University, Taiwan. From 1985 to 1991, he was an assistant researcher and an instrumentation system engineer of the Flight Test Group, Aeronautic Research Laboratory, Zhong Shan Institute of Science and Technology, Taiwan. Since 1991, he has been with the Department of Mechanical Engineering at National Chin Yi University of Technology, Taiwan. His research interests are in reliability engineering, data acquisition system, biomedical engineering (cardiac pacemakers, patient nursing monitoring, otolith restoration, and drunk-driving prevention), and automation.
(skyang@ncut.edu.tw)



**Yi-Ting Tsai** received her M.S. degree in mechanical in 2024 engineering from National Chin Yi University of Technology, Taiwan. Her research interests are in failure prediction, reliability engineering, and automation. (annabox@yahoo.com.tw)



**Kai-Jung Chen** is an accomplished individual with a bachelor's degree in engineering (2010) and a master's degree in biomechanical engineering (2012) from National Cheng Kung University in Taiwan, and a Ph.D. degree in engineering from the University of Liverpool, UK (2019). From 2014 to 2019, he played a pivotal role in the Biomechanical Engineering Group at the University of Liverpool, focusing on precision ophthalmic equipment development. Since 2020, Kai-Jung has been a faculty member in the Department of Mechanical Engineering at National Chin-Yi University of Technology, Taiwan. His diverse research interests include computational biomechanics, medical assistive device development, big data and AI technology, and semiconductor and brittle material processing.
(hskchen5@ncut.edu.tw)